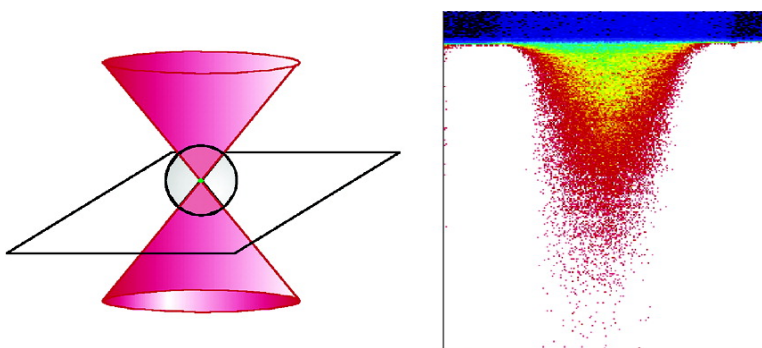


## In Situ Observation of Molecular Diffusion in Solid Supports Using Two-Photon Fluorescence Microscopy

Mariko M. Taniguchi, Richard A. Farrer, and John T. Fourkas

*J. Comb. Chem.*, **2005**, 7 (1), 54-57 • DOI: 10.1021/cc049896k • Publication Date (Web): 18 November 2004

Downloaded from <http://pubs.acs.org> on March 22, 2009



### More About This Article

Additional resources and features associated with this article are available within the HTML version:

- Supporting Information
- Links to the 2 articles that cite this article, as of the time of this article download
- Access to high resolution figures
- Links to articles and content related to this article
- Copyright permission to reproduce figures and/or text from this article

[View the Full Text HTML](#)



**ACS Publications**  
High quality. High impact.

# In Situ Observation of Molecular Diffusion in Solid Supports Using Two-Photon Fluorescence Microscopy

Mariko M. Taniguchi, Richard A. Farrer, and John T. Fourkas\*

*Eugene F. Merkert Chemistry Center, Boston College, Chestnut Hill, Massachusetts 02467*

*Received June 16, 2004*

We demonstrate that two-photon fluorescence microscopy is a useful tool for monitoring the diffusion of molecules through polymeric solid supports. As a proof of principle, TentaGel beads were bound to a cover slip, and diffusion of Rhodamine 6G through single beads was observed in real time. Diffusion experiments performed in 40 different beads indicate that there is a considerable degree of heterogeneity in diffusion rates from bead to bead.

## Introduction

The introduction of techniques that utilize solid supports<sup>1</sup> has had a large impact on chemical synthesis, particularly as applied to combinatorial chemistry. The microscopic physical properties of the supports play a key role in solid-phase synthesis, and developing a better understanding of these properties is vital if we are to be able to take full advantage of the potential of this technique. However, relatively little work has been done to understand the properties of synthesis resins in a systematic fashion. Attempts at comprehensive understanding of the physical properties of these resins are largely limited to collected information in review articles.<sup>2–4</sup> This current level of understanding is inadequate for the expanding role of solid support techniques throughout the sciences, since it is largely gathered from investigations that are tailored for a specific reaction type.

A key physical property of synthesis resins is the ability of reagents and reaction products to diffuse throughout the polymer matrix. The rate of diffusion depends on the solvent employed, the identity of the diffusing species, and the collective properties of the resin and any molecules that have been bound to it. It is, therefore, desirable to be able to understand how diffusion of molecules through solid supports depends on all of these parameters. Previous studies of the diffusive properties of synthesis resins have fallen into two basic categories. In the first type of experiment, self-diffusion of solvent molecules is measured using pulsed-field gradient NMR methods.<sup>5,6</sup> This approach requires a high concentration of diffusing molecules and so cannot directly provide an understanding of how reactants and products can diffuse through the polymeric matrix. In the second type of study, diffusion of reagents is allowed to proceed for a set period of time, after which the extent of diffusion is visualized.<sup>7,8</sup> However, there is a considerable degree of heterogeneity both within and between individual polymer beads, which makes

it difficult to develop a comprehensive picture of the diffusion process using static snapshots.

Two-photon fluorescence microscopy (TPFM)<sup>9,10</sup> is an increasingly popular technique for performing cross-sectional imaging of fluorescent objects. In this technique, two photons of near-infrared laser radiation are used to excite a fluorophore that has a single-photon absorption in the visible region of the spectrum. Because both photons must be present at the same place at the same time for absorption to occur, the absorption probability is proportional to the square of the laser intensity. As a result, excitation can be limited to within the focal volume of a laser that has been focused through a microscope objective. Thus, by moving the position of this focal volume in three dimensions, cross-sectional fluorescence images of an object can be obtained.

TPFM is suited ideally to obtaining images of the interiors of synthesis beads. The high spatial resolution of TPFM allows for detailed imaging of individual beads, and the beads themselves are generally highly transparent to near-infrared radiation. We have previously reported the use of TPFM to observe spatially dependent properties of synthesis beads,<sup>8</sup> and others have subsequently used this technique to quantify the loading of individual beads<sup>11</sup> and to monitor enzymatic reaction rates.<sup>12</sup> Here, we report the application of this technique to the in situ, real-time observation of diffusion of molecules in individual synthesis beads.

## Results and Discussion

TPFM has been used previously to study diffusion using the fluorescence recovery after photobleach (FRAP) technique.<sup>13</sup> FRAP experiments begin with an equilibrated distribution of dye molecules. The laser beam focus is fixed at a particular position in the sample, and dye molecules are bleached at high power. One- or two-dimensional scans are then performed at low intensity to monitor the recovery of fluorescence in the bleached region, which occurs via diffusion. We have found that high laser intensities can cause photochemical reactions in polystyrene-based resins. We

\* To whom correspondence should be addressed. E-mail: fourkas@bc.edu.

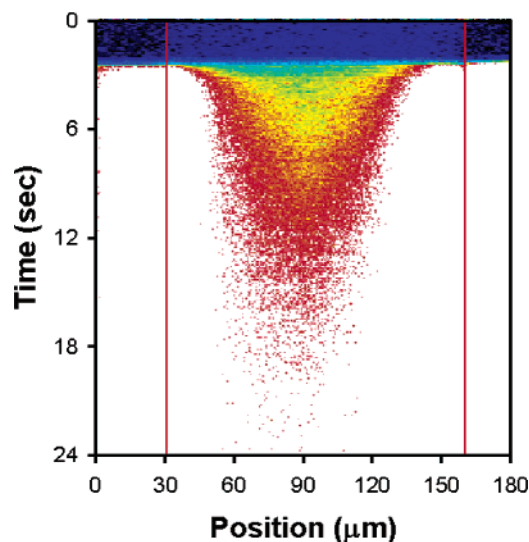


**Figure 1.** Representative false-color image of diffusion of a dye solution into a single bead. The horizontal dimension corresponds to position along a horizontal line through the center of the bead, and the vertical axis corresponds to time. White corresponds to the highest number fluorescence counts and black to the smallest number. The sudden transition in fluorescence counts outside the bead at  $\sim 2.5$  s is due to the addition of the dye solution to the cell. The vertical red lines denote the edges of the microsphere.

chose instead to begin with beads that did not initially contain dye and to monitor the diffusion of fluorescent molecules into them, which can be accomplished at low laser intensities.

Because of its widespread use in solid-phase combinatorial synthesis, we chose to study diffusion in amine-functionalized, high-loading TentaGel resin (Rapp Polymere GmbH). To immobilize beads so that diffusion could be monitored, they were bound covalently to microscope cover slips. Individual cover slips were placed in a leak-proof sample holder that fits on the stage of an inverted two-photon microscope, and dimethylformamide (DMF) was added to swell the beads. Preswelling was employed both because it is a typical step in syntheses on solid supports and because it allows the dye to diffuse into the supports, as opposed to being forced in by the solvent as the supports solvate. The slight intrinsic fluorescence of the resin is used to locate a single bead on the microscope. Once the center of the bead has been located, a set of scans along a horizontal line through the center of the bead is performed to assess the intrinsic background fluorescence. Once the background fluorescence has been determined, a solution of Rhodamine 6G (R6G) in DMF is injected quickly into the sample cell. Line scans are used to monitor the diffusion of the fluorophore into the bead (Figure 1). A final set of line scans is obtained after diffusion is complete to determine the maximum fluorescence accurately. Once all of the scans have been collected, the average background is subtracted from the data, and then the data are normalized to the average final intensity.

As a model for the diffusive process, we consider the free solution to be a large enough reservoir for the fluorophore that its concentration in the free solution remains constant through the diffusion process. If we ignore the curvature of the beads, we can employ a model that is commonly used in modeling the doping dynamics of semiconductors.<sup>14,15</sup>

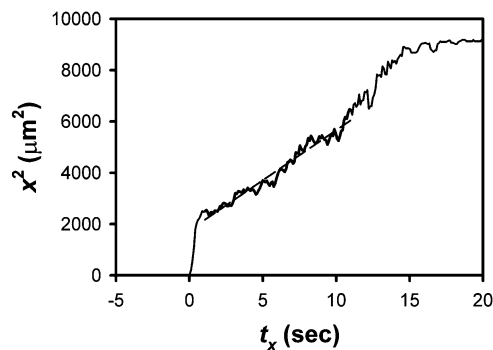


**Figure 2.** Representative plot of  $x^2$  as a function of  $t_x$  for a single bead. The data in this plot were subjected to a rolling average over seven pixels. The dye solution was added at time 0. Dye diffuses rapidly into the less dense outer portion of the bead, at times ranging between  $\sim 0$  and 1 s. After this rapid initial diffusion,  $x^2$  grows linearly with  $t_x$  for a substantial period of time; the dashed line in the plot is a linear least-squares fit to data between 1 and 11 s that was used to determine the diffusion constant for this bead. As diffusion proceeds further, both the spherical geometry of the bead and the finite size of the probed volume contribute to making  $x^2$  grow superlinearly with  $t_x$ . Diffusion is complete at  $\sim 15$  s.

According to this model, the concentration of fluorophore at distance  $x$  from the edge of the bead should follow

$$\frac{C_x(t) - C_x(0)}{C_s - C_x(0)} = \operatorname{erfc}\left(\frac{x}{2\sqrt{Dt}}\right) \quad (1)$$

where  $C_s$  is the constant concentration of fluorophore in the solution,  $C_x$  is the concentration of fluorophore at position  $x$  in the bead,  $t$  is the time elapsed since addition of the fluorophore,  $D$  is the diffusion constant, and  $\operatorname{erfc}$  is the complementary error function. Since the resin beads initially are swollen only with solvent,  $C_x(0)$  is equal to zero, and the left-hand side of this equation is reduced to a ratio of the concentration of fluorophore at a given distance inside the matrix to that in the solution. We denote this relative fluorescence intensity  $I_x(t)$ .

The diffusion data are analyzed by picking a particular threshold value of  $I_x(t)$  and finding at what time,  $t_x$ , this intensity is attained as a function of  $x$ . There is a unique value of the argument of the complementary error function, which we will denote  $k$ , that corresponds to any chosen threshold value of  $I_x$ . The diffusion constant, therefore, follows the relation

$$D = \frac{x^2}{4k^2 t_x} \quad (2)$$

Thus, according to this model, a plot of  $x^2$  as a function of  $t_x$  should be linear with a slope of  $4Dk^2$ .

A typical plot of  $x^2$  versus  $t_x$  is shown in Figure 2. The relative intensity threshold chosen here was 0.8. Other threshold values give similar results, but thresholds in this range were found to give the greatest degree of consistency. Note that  $x^2$  is not a linear function of  $t_x$  over the full range of positions in the bead. This is to be expected, since the bead is spherical; the closer one gets to the center of the bead, the more the planar approximation used in the above derivation breaks down, and the more important the thickness of the cross-section that is probed by the laser becomes. In

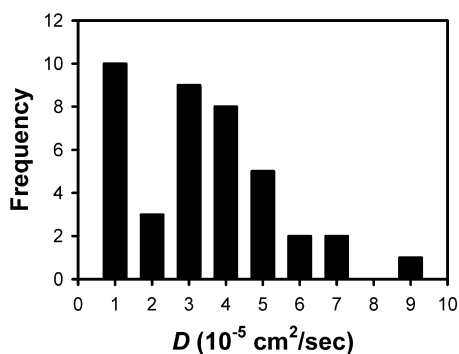


**Figure 3.** Histogram of the occurrences of different values of diffusion constants for the 40 beads studied here.

addition, the polymer density at the outside of a bead is significantly less than that throughout the remainder of the bead, and so diffusion occurs very quickly in this outermost region. Between these extremes there is a region in which  $x^2$  grows linearly with  $t_x$ , and it is the data in this region that are used to determine  $D$ .

Shown in Figure 3 is a histogram of diffusion constants measured in 40 individual beads. The average diffusion constant for these beads is  $3.9 \times 10^{-5} \text{ cm}^2/\text{s}$ . This average diffusion constant is on the same order of magnitude as would be expected in the bulk solvent, which is not surprising on the basis of the relatively low degree of cross-linking of the resin and its high degree of swelling in DMF. As is clear from Figure 3, there is a significant spread in the measured diffusion constants. Indeed, the standard deviation for these data is  $1.9 \times 10^{-5} \text{ cm}^2/\text{s}$ , which is more than one-half of the average diffusion constant. It is also noteworthy that the distribution is quite asymmetric, with lower values being more prevalent than larger values. Although it is possible that some of this spread arises from slight variations in experimental conditions from run to run, it is clear, nevertheless, that there are significant differences in diffusive behavior that can be observed from bead to bead.

### Conclusions

We have demonstrated that TPFM is a valuable technique for studying the diffusive properties of molecules within solvent-swollen solid-supports. The results of this proof-of-principle study demonstrate that there is significant heterogeneity in the diffusive properties of individual high-loading TentaGel beads. Our method is quite general and can readily be extended to other supports, solvents, and fluorescent diffusing species. It will also be of great interest to study how diffusive properties change with the size and nature of molecules bound to a resin. Information from such studies would help us to gain insight into how synthetic conditions should be varied to optimize the yield at each step as peptides are synthesized on solid support, for instance.

### Experimental Section

**Two-Photon Fluorescence Microscope.** Our system has been described in detail elsewhere.<sup>16</sup> A commercial Ti:sapphire laser (Coherent Mira Basic) is pumped by a diode-pumped solid-state laser (Coherent Verdi 5). The Ti:sapphire produces 80-fs pulses with a center wavelength of 800 nm

at a repetition rate of 76 MHz. The laser output is reflected off two galvanometric scanning mirrors and into the reflected-light port of an inverted microscope (Zeiss Axiovert S100 TV). The laser beam is then reflected from a dichroic mirror and focused through the objective into a sample. The objective employed is either a 10 $\times$  with an NA of 0.3 (Zeiss Neofluar) or a 20 $\times$  with an NA of 0.5 (Zeiss Neofluar). Any resultant fluorescence is collected through the same objective, after which it passes through the dichroic mirror and a set of filters that remove any scattered excitation light. The fluorescence is collected by a pair of low-background avalanche photodiodes that are set up to detect opposite polarizations of light. For all of the data reported here, the outputs of the two photodiodes were added together. The galvanometric scanning mirrors were used to control the position of the focus in the  $x$ - $y$  plane of the sample during image acquisition, and the three-dimensional positioning of the sample was controlled by a motorized stage and a focusing drive (Ludl BioPrecision).

**Modification of Cover Slips.** Glass cover slips (Fisher brand no. 1) were prepared for modification by soaking in a 3:1 solution of concentrated sulfuric acid and 30% hydrogen peroxide for 24 h. [Caution: this solution is highly oxidizing and should be handled accordingly.] The surfaces were then modified with 3-aminopropyltriethoxysilane<sup>17</sup> by suspending the cover slips for 5 min in a 2% solution (by volume) of the silane in ethanol. The slips were then gently rinsed with ethanol and allowed to dry for 15 min at 110  $^{\circ}\text{C}$ .

**Attachment of Beads.** Once cooled, the cover slips were soaked for 12 h in DMF containing an excess of 1,4,5,8-naphthalene-tetracarboxylic dianhydride. After drying, the cover slips were placed in a suspension of amine-functionalized (0.43 mmol/g) 90- $\mu\text{m}$ -diameter TentaGel beads in DMF that had mixed previously in a spin tube for at least 2 h. Binding was allowed to proceed over a period of 3 days, after which the cover slips were lightly rinsed with solvent (DMF) to remove any unbound beads. The cover slips were then allowed to dry at room temperature. Each bead-modified cover slip was used only once, since attempts to reuse samples revealed that significant traces of fluorophore remain in the resin matrix, even after extensive washing.

**Sample Preparation.** The sample cell consisted of a brass plate the size of a microscope slide with a depression in it the size of a cover slip and an aperture in the center of the depression for imaging. A second, smaller brass plate with an aperture can be bolted on top of the first plate, and a Teflon block with a cylindrical hole with a volume of  $\sim 2$  mL can be sandwiched between them. The first time it is used, the Teflon block is sandwiched between two clean cover slips, and the entire assembly is heated to a temperature at which the Teflon becomes slightly soft. This procedure helps to smooth out any surface roughness in the Teflon. For the experiments reported here, a bead-modified cover slip was placed on the bottom plate, bead side up, and the Teflon block was affixed to it and sealed using Silicone II (General Electric). The sealant is allowed to cure for at least 24 h, after which the cell is filled with DMF. Prior to use, the solvent is decanted from the cell, and 200  $\mu\text{L}$  of fresh



DMF is added to the cell and allowed to equilibrate for 1 h to ensure that the beads remain swollen.

**Data Acquisition.** Acquisition of data occurred in a temperature- and humidity-controlled environment. The sample cell was allowed to equilibrate on the microscope stage for at least 10 min. The scanning rate was set such that the diffusive front penetrates to the center of the sphere within one scan screen (256 line scans). A 1-mL aliquot of a  $5 \times 10^{-5}$  M solution of R6G in DMF was added to the sample cell using a 10-mL syringe. The injection syringe was located outside the microscope box, and the fluorescent solution was transferred through Teflon tubing that was threaded through a small opening into the box. The tubing was then directed into the sample cell and held in place by a guide. Migration of fluorophore was observed by scanning the focal point of the laser beam along a horizontal line through the center of the microsphere, which was first centered on the scanning screen.

**Data Analysis.** Data sets are in the form of  $256 \times 256$  arrays of pixels in which one dimension is position and the other is time. The average background prior to the addition of the dye solution is subtracted from the data, which are then normalized to the average intensity after diffusion is complete. A relative intensity threshold is chosen, and then a computer program determines the time for which this threshold is attained for each position within a bead. These data are then converted into a plot of  $x^2$  as a function of  $t_x$ , as in Figure 2. If necessary, the data are smoothed with a rolling average, and then the time window in which  $x^2$  varies linearly with  $t_x$  is determined. Linear least-squares fitting is used to find the slope in this region, and thereby determine the diffusion coefficient.

**Acknowledgment.** This work was supported by the National Science Foundation, Grants CHE-0073228 and

CHE-0314020. J.T.F. is a Research Corporation Cottrell Scholar and a Camille Dreyfus Teacher-Scholar.

## References and Notes

- (1) Merrifield, R. B. *J. Am. Chem. Soc.* **1963**, *85*, 2149–2154.
- (2) Meldal, M. *Methods Enzymol.* **1997**, *289*, 83–104.
- (3) Sherrington, D. C. *Chem. Commun.* **1998**, 2275–2286.
- (4) Vaino, A. R.; Janda, K. D. *J. Comb. Chem.* **2000**, *2*, 579–596.
- (5) Ford, W. T.; Ackerson, B. J.; Blum, F. D.; Periyasamy, M.; Pickup, S. *J. Am. Chem. Soc.* **1987**, *109*, 7276–7280.
- (6) Pickup, S.; Blum, F. D.; Ford, W. T.; Periyasamy, M. *J. Am. Chem. Soc.* **1986**, *108*, 3987–3990.
- (7) Groth, T.; Groth, M.; Meldal, M. *J. Comb. Chem.* **2001**, *3*, 461–468.
- (8) Farrer, R. A.; Copeland, G. T.; Previte, M. J. R.; Okamoto, M. M.; Miller, S. J.; Fourkas, J. T. *J. Am. Chem. Soc.* **2002**, *124*, 1994–2003.
- (9) Denk, W.; Strickler, J. H.; Webb, W. *Science* **1990**, *248*, 73–76.
- (10) So, P. T. C.; Dong, C. Y.; Masters, B. R.; Berland, K. M. *Annu. Rev. Biomed. Eng.* **2000**, *2*, 399–429.
- (11) Ulijn, R. V.; Brazendale, I.; Margetts, G.; Flitsch, S. L.; McConnell, G.; Girkin, J.; Halling, P. J. *J. Comb. Chem.* **2003**, *5*, 215–217.
- (12) Bosma, A. Y.; Ulijn, R. V.; McConnell, G.; Girkin, J.; Halling, P. J.; Flitsch, S. L. *Chem. Commun.* **2003**, 2790–2791.
- (13) Brown, E. B.; Wu, E. S.; Zipfel, W.; Webb, W. W. *Biophys. J.* **1999**, *77*, 2837–2849.
- (14) Helfferich, F. G. *Ion Exchange*; McGraw-Hill: New York, 1962.
- (15) Crank, J. *The Mathematics of Diffusion*; Clarendon Press: Oxford, UK, 1956.
- (16) Farrer, R. A.; Previte, M. J. R.; Olson, C. E.; Peyser, L. A.; Fourkas, J. T.; So, P. T. C. *Opt. Lett.* **1999**, *24*, 1832–1834.
- (17) Arkles, B. *Chemtech* **1977**, *7*, 766.

CC049896K